Testing the standard model with $D_{(s)} \to K_1(\to K\pi\pi)\gamma$ decays

Nico Adolph,* Gudrun Hiller,† and Andrey Tayduganov‡
Fakultät Physik, TU Dortmund, Otto-Hahn-Str.4, D-44221 Dortmund, Germany

(Received 18 December 2018; published 17 April 2019)

The photon polarization in $D_{(s)} \to K_1(\to K\pi\pi)\gamma$ decays can be extracted from an up-down asymmetry in the $K\pi\pi$ system, along the lines of the method known to $B \to K_1(\to K\pi\pi)\gamma$ decays. Charm physics is advantageous as partner decays exist: $D^+ \to K_1^+(\to K\pi\pi)\gamma$, which is standard model-like, and $D_s \to K_1^+(\to K\pi\pi)\gamma$, which is sensitive to physics beyond the standard model in $|\Delta c| = |\Delta u| = 1$ transitions. The standard model predicts their photon polarizations to be equal up to U-spin breaking corrections, while new physics in the dipole operators can split them apart at order one level. We estimate the proportionality factor in the asymmetry multiplying the polarization parameter from axial vectors $K_1(1270)$ and $K_1(1400)$, and find it to be sizable, up to the few $\mathcal{O}(10)\%$ range. The actual value of the hadronic factor matters for the experimental sensitivity but is not needed as an input to perform the null test.

DOI: 10.1103/PhysRevD.99.075023

I. INTRODUCTION

Charm decay amplitudes are notoriously challenging due to an often overwhelming resonance contribution in addition to poor convergence of the heavy quark expansion. Yet, rare charm decays are of particular importance as they are sensitive to flavor and CP violation in the up sector, complementary to K- and B-physics. While the number of radiative and semileptonic $|\Delta c| = |\Delta u| = 1$ modes within reach of the flavor facilities *BABAR*, Belle, LHCb, BESIII, and Belle II is plenty, it needs dedicated efforts to get sufficient control over hadronic uncertainties to be able to test the standard model (SM). A useful strategy known as well to the presently much more advanced B-physics program is to custom-build observables "null tests," exploiting approximate symmetries of the SM, such as lepton universality, CP in $b \to s$ and $c \to u$ transitions, or $SU(3)_F$. This allows one to bypass a precise, first-principle computation of hadronic matrix elements which presently may not exist.

In this work, we provide a detailed study of the up-down asymmetry $\mathcal{A}_{\rm UD}$ in the angular distributions of $D^+ \to K_1^+(\to K\pi\pi)\gamma$ and $D_s \to K_1^+(\to K\pi\pi)\gamma$ decays, as a means to test the SM. Originally proposed for B decays [1,2], the method is advantageous in charm as one does not have to rely on prior knowledge of the $K\pi\pi$ spectrum and theory predictions of the photon polarization. Instead, one can use the fact that the spectrum is universal and the photon polarizations of D^+ and D_s decays in the SM are identical in the U-spin limit [3].

Both $D_{(s)} \to K_1^+\gamma$ decays are color allowed and are induced by W-exchange "weak annihilation" (WA), which is doubly Cabibbo suppressed and singly Cabibbo suppressed in D^+ and D_s decays, respectively. Thus, the ratio of their branching fractions $\mathcal{B}(D^+ \to K_1^+\gamma)/\mathcal{B}(D_s \to K_1^+\gamma) \approx |V_{cd}/V_{cs}|^2(\tau_D/\tau_{D_s})$ is about 0.1, taking into account the different Cabibbo-Kobayashi-Maskawa elements V_{ij} and lifetimes $\tau_{D_{(s)}}$ [4]. While the D^+ decay is SM-like, the D_s decay is a flavor changing neutral current (FCNC) process and is sensitive to physics beyond the SM (BSM) in photonic dipole operators, which can alter the polarization. The photon dipole contributions in the SM are negligible due to the Glashow-Iliopoulos-Maiani (GIM) mechanism. The photon polarization in the SM in $c \to u\gamma$ is predominantly left handed; however, in the D-meson decays, sizable hadronic corrections are expected [3,5–7]. In the proposal discussed in this work, the polarization is extracted from the SM-like decay $D^+ \to K_1^+\gamma$. We test the SM by comparison to the photon polarization in $D_s \to K_1^+\gamma$ decays. Methods to look for new physics (NP) with the photon polarization in $c \to u\gamma$ transitions have been studied recently in Refs. [3,8].

The plan of the paper is as follows. General features of the decays $D^+ \to K_1^+\gamma$ and $D_s \to K_1^+\gamma$ are discussed in Sec. II, including angular distributions for an axial-vector K_1^+ decaying to $K\pi\pi$. Predictions in the framework of QCD factorization [9,10] are given and used to estimate the $D^+, D_s \to K_1^+\gamma$ branching ratios, which are not measured.

*nico.adolph@tu-dortmund.de
†ghiller@physik.uni-dortmund.de
‡andrey.tayduganov@tu-dortmund.de

We stress that the SM null test proposed in this paper does not rely on theoretical calculations of rare charm decay amplitudes. We circumvent a SM calculation of the photon polarization by an experimental determination in a SM-like decay, $D^+ \to K_1^+\gamma$. In Sec. III, we analyze $K_1^+ \to K^+\pi^+\pi^-$ and $K_1^+ \to K^0\pi^+\pi^0$ decay chains. Phenomenological profiles of the up-down asymmetry are worked out in Sec. IV. In Sec. V, we conclude. Auxiliary information is given in three Appendixes.

II. DECAYS $D^+ \to K_1^+\gamma$ AND $D_s \to K_1^+\gamma$

In Sec. II A, we give the $D_{(s)} \to K_1(\to K\pi\pi)\gamma$ angular distribution that allows us to probe the photon polarizations and perform the null test. In Sec. II B, we discuss dominant SM amplitudes and estimate the $D_{(s)} \to K_1(1270)\gamma$ and $D_{(s)} \to K_1(1400)\gamma$ branching ratios. The BSM reach is investigated in Sec. II C.

A. $D_{(s)} \to K_1(\to K\pi\pi)\gamma$ angular distribution

The $D_{(s)} \to K_1\gamma$ decay rate, where K_1 is an axial-vector meson, can be written as [11]

$$\Gamma^{D_{(s)}} = \frac{\alpha_e G_F^2 m_{D_{(s)}}^3}{32\pi^4}\left(1-\frac{m_{K_1}^2}{m_{D_{(s)}}^2}\right)^3 (|A_L^{D_{(s)}}|^2 + |A_R^{D_{(s)}}|^2), \quad (1)$$

where L, R refers to the photon's left-handed, right-handed polarisation state, respectively. Here, G_F denotes Fermi's constant, and α_e is the fine structure constant. $A_{L,R}^{D_{(s)}}$ denote the $D_{(s)} \to K_1\gamma$ decay amplitudes.

The polarization parameter $\lambda_\gamma^{D_{(s)}}$ is defined as

$$\lambda_\gamma^{D_{(s)}} = -\frac{1-r_{D_{(s)}}^2}{1+r_{D_{(s)}}^2}, \qquad r_{D_{(s)}} = \left|\frac{A_R^{D_{(s)}}}{A_L^{D_{(s)}}}\right| \quad (2)$$

and can be extracted from the angular distribution in $D_{(s)} \to K_1(\to K\pi\pi)\gamma$ decays

$$\frac{\mathrm{d}^4\Gamma^{D_{(s)}}}{\mathrm{d}s\mathrm{d}s_{13}\mathrm{d}s_{23}\mathrm{d}\cos\theta} \propto \{|\mathcal{J}|^2(1+\cos^2\theta) + \lambda_\gamma^{D_{(s)}} 2\mathcal{I}m[\vec{n}\cdot(\vec{\mathcal{J}}\times\vec{\mathcal{J}}^*)]\cos\theta\}\mathrm{PS}^{D_{(s)}}, \quad (3)$$

with the phase space factor

$$\mathrm{PS}^{D_{(s)}} = \frac{1-s/m_{D_{(s)}}^2}{256(2\pi)^5 m_{D_{(s)}} s}. \quad (4)$$

Here, s denotes the $K\pi\pi$ invariant mass squared, needed for finite width effects; θ is the angle between the normal $\vec{n} = (\vec{p}_1\times\vec{p}_2)/|\vec{p}_1\times\vec{p}_2|$ and the direction opposite to the photon momentum in the rest frame of the K_1; and $s_{ij} = (p_i+p_j)^2$ with 4-momenta p_i of the final pseudoscalars with assignments specified in (18). Note that p_3 refers to the K's momentum. Furthermore, $\mathcal{J}$ is a helicity amplitude defined by the decay amplitude $A(K_1 \to K\pi\pi) \propto \varepsilon^\mu \mathcal{J}_\mu$ with a polarization vector ε of the K_1; see Sec. III for details. $\vec{\mathcal{J}}$ are the spacial components of the 4-vector $\mathcal{J}$. $\mathcal{J}$ is a feature of the resonance decay, and as such, it is universal for D^+ and D_s decays.

From (3), one can define an integrated up-down asymmetry which is proportional to the polarization parameter,

$$\mathcal{A}_{\mathrm{UD}}^{D_{(s)}} = \left(\int_0^1 \frac{\mathrm{d}^2\Gamma}{\mathrm{d}s\mathrm{d}\cos\theta}\mathrm{d}\cos\theta - \int_{-1}^0 \frac{\mathrm{d}^2\Gamma}{\mathrm{d}s\mathrm{d}\cos\theta}\mathrm{d}\cos\theta\right)\Big/ \int_{-1}^1 \frac{\mathrm{d}^2\Gamma}{\mathrm{d}s\mathrm{d}\cos\theta}\mathrm{d}\cos\theta = \frac{3}{4}\frac{\langle\mathcal{I}m[\vec{n}\cdot(\vec{\mathcal{J}}\times\vec{\mathcal{J}}^*)]\kappa\rangle}{\langle|\vec{\mathcal{J}}|^2\rangle}\lambda_\gamma^{D_{(s)}}, \quad (5)$$

where $\kappa = \mathrm{sgn}[s_{13}-s_{23}]$ for $K_1^+ \to K^0\pi^+\pi^0$ and $\kappa = 1$ for $K_1^+ \to K^+\pi^+\pi^-$. The brackets $\langle\ldots\rangle$ denote integration over s_{13} and s_{23}. The reason for introducing κ is explained in Sec III. The up-down asymmetry is maximal for maximally polarized photons, purely left-handed, $\lambda_\gamma^{D_{(s)}} = -1$, or purely right-handed ones, $\lambda_\gamma^{D_{(s)}} = +1$.

It is clear from Eqs. (3) and (5) that the sensitivity to the photon polarization parameter $\lambda_\gamma^{D_{(s)}}$ depends on $\mathcal{I}m[\vec{n}\cdot(\vec{\mathcal{J}}\times\vec{\mathcal{J}}^*)]$. If this factor is zero, or too small, we have no access to $\lambda_\gamma^{D_{(s)}}$. As the $\mathcal{J}$-amplitudes are the same for D^+ and D_s, the factor drops out from the ratio

$$\frac{\mathcal{A}_{\mathrm{UD}}^{D^+}}{\mathcal{A}_{\mathrm{UD}}^{D_s}} = \frac{\lambda_\gamma^{D^+}}{\lambda_\gamma^{D_s}} = \frac{1-r_{D^+}^2}{1+r_{D^+}^2}\frac{1+r_{D_s}^2}{1-r_{D_s}^2}. \quad (6)$$

In the SM, this ratio equals 1 in the U-spin limit. Corrections are discussed in Sec. II B.

In general, there is more than one K_1 resonance contributing to $K\pi\pi$, such as $K_1(1270)$ and $K_1(1400)$. Note that the phase space suppression for the $K_J(1400)$-family and higher with respect to the $K_1(1270)$ is stronger in charm than in B decays. Therefore, a single- or double-resonance ansatz with the $K_1(1270)$ or $K_1(1400)$ is in better shape than in the corresponding $B \to K_1(\to K\pi\pi)\gamma$ decays. In the presence of more than one overlapping K_1 resonance, beyond the zero-width approximation, the relation between the polarization and the up-down asymmetry gets more complicated than (5). The reason is that, ultimately, $r_{D_{(s)}}$ and the polarization are different for $K_1(1270)$ and $K_1(1400)$; that is, they vary with s, an effect that can be controlled by cuts. The general formula can be seen in Appendix C. What stays intact, however, is the SM prediction, $(\mathcal{A}_{\mathrm{UD}}^{D^+}/\mathcal{A}_{\mathrm{UD}}^{D_s})_{\mathrm{SM}} = 1$ up to U-spin breaking.

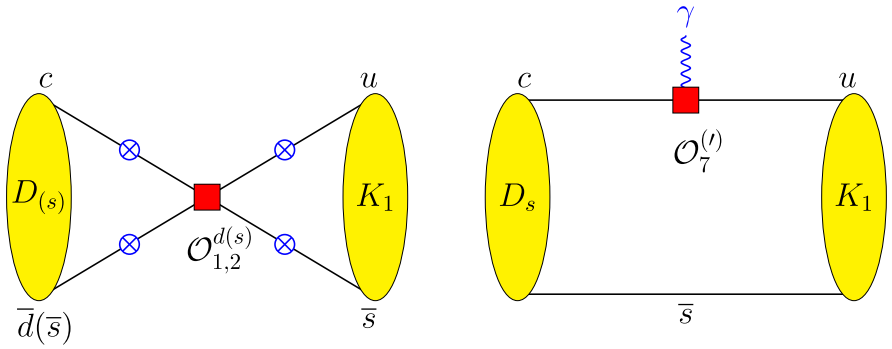

FIG. 1. Weak annihilation (left) and photon dipole (right) contributions to $D_{(s)} \to K_1\gamma$ decays. In the weak annihilation diagram, the crosses indicate where the photon can be attached.

B. SM

Rare $c \to u\gamma$ processes can be described by the effective Hamiltonian [11,12],

$$\mathcal{H}_{\rm eff} = -\frac{4G_F}{\sqrt{2}}\left[\sum_{q=d,s} V_{cq}^* V_{uq} \sum_{i=1}^{2} C_i \mathcal{O}_i^q + V_{cd}^* V_{us}\, C_2 \mathcal{O}_2^{ds} + \sum_{i=3}^{6} C_i \mathcal{O}_i + \sum_{i=7}^{8} (C_i \mathcal{O}_i + C_i' \mathcal{O}_i')\right], \tag{7}$$

where the operators relevant to this work are defined as follows,

$$\begin{aligned} \mathcal{O}_1^{q=d,s} &= (\bar{u}_L \gamma_\mu T^a q_L)(\bar{q}_L \gamma^\mu T^a c_L), \\ \mathcal{O}_2^{q=d,s} &= (\bar{u}_L \gamma_\mu q_L)(\bar{q}_L \gamma^\mu c_L), \\ \mathcal{O}_2^{ds} &= (\bar{u}_L \gamma_\mu s_L)(\bar{d}_L \gamma^\mu c_L), \\ \mathcal{O}_7 &= \frac{e}{16\pi^2} m_c \bar{u}_L \sigma^{\mu\nu} c_R F_{\mu\nu}, \\ \mathcal{O}_7' &= \frac{e}{16\pi^2} m_c \bar{u}_R \sigma^{\mu\nu} c_L F_{\mu\nu}, \end{aligned} \tag{8}$$

with chiral left (right) projectors L (R); the field strength tensor of the photon, $F_{\mu\nu}$; and the generators of $SU(3)_c$, T^a, $a = 1, 2, 3$. Contributions to $D_{(s)} \to K_1\gamma$ decays are illustrated in Fig. 1.

In the SM, both four-quark operators $\mathcal{O}_{1,2}$ are induced at tree level and acquire order one coefficients at the charm quark mass m_c. On the other hand, the SM contributions to the dipole operators $\mathcal{O}_7^{(\prime)}$ are strongly GIM suppressed, $C_7^{\rm eff} \in [-1.51 - 5.51i, -0.88 - 3.25i] \times 10^{-3}$, at two loop level [11], and $C_7' \sim m_u/m_c \simeq 0$. The $D^+ \to K_1^+\gamma$ and $D_s \to K_1^+\gamma$ decays are therefore expected to be dominated by the four-quark operators.

We employ QCD factorization methods [10] to estimate the $D^+, D_s \to K_1^+\gamma$ branching ratios, which presently are not known otherwise. We stress that we do not rely on these predictions in the SM null test we are proposing. On the other hand, the study of QCD factorization amplitudes in D decays can give quantitative information on the performance of the framework once data are available, which is useful in B-physics, where corrections are less pronounced. The leading SM contribution to $D_{(s)} \to K_1\gamma$ decays is shown in the diagram to the left in Fig. 1, with the radiation of the photon from the light quark of the $D_{(s)}$ meson. The other three WA diagrams are suppressed by $\Lambda_{\rm QCD}/m_c$ and are neglected. The corresponding WA amplitudes for $D \to V\gamma$ have been computed in Ref. [11]. We obtain[1]

$$\begin{aligned} A_{L\,\rm SM}^{D} &= -\frac{2\pi^2 Q_d f_D f_{K_1} m_{K_1}}{m_D \lambda_D} V_{cd}^* V_{us} C_2 \frac{m_D^2}{m_D^2 - m_{K_1}^2}, \\ A_{L\,\rm SM}^{D_s} &= -\frac{2\pi^2 Q_d f_{D_s} f_{K_1} m_{K_1}}{m_{D_s} \lambda_{D_s}} V_{cs}^* V_{us} C_2 \frac{m_{D_s}^2}{m_{D_s}^2 - m_{K_1}^2}, \end{aligned} \tag{9}$$

where $Q_d = -1/3$. We also kept explicitly, i.e., did not expand in $1/m_D$, the factors that correct for the kinematic factors in $\Gamma^{D_{(s)}}$, see (1), corresponding to the matrix elements of dipole operators. Due to the low value of the charm scale, one expects sizable corrections to the $1/m_c$ and α_s expansion. Using the range $C_2 \in [1.06, 1.14]$ [11], we find

$$\begin{aligned} \mathcal{B}(D^+ \to K_1^+(1270)\gamma) &= [(1.3 \pm 0.3), (1.5 \pm 0.4)] \times 10^{-5} \left(\frac{0.1\ \text{GeV}}{\lambda_D}\right)^2, \\ \mathcal{B}(D^+ \to K_1^+(1400)\gamma) &= [(1.4 \pm 0.6), (1.6 \pm 0.7)] \times 10^{-5} \left(\frac{0.1\ \text{GeV}}{\lambda_D}\right)^2, \\ \mathcal{B}(D_s \to K_1^+(1270)\gamma) &= [(1.9 \pm 0.4), (2.2 \pm 0.5)] \times 10^{-4} \left(\frac{0.1\ \text{GeV}}{\lambda_{D_s}}\right)^2, \\ \mathcal{B}(D_s \to K_1^+(1400)\gamma) &= [(2.0 \pm 0.9), (2.4 \pm 1.0)] \times 10^{-4} \left(\frac{0.1\ \text{GeV}}{\lambda_{D_s}}\right)^2, \end{aligned} \tag{10}$$

[1]There is a minus sign for axial vectors relative to vector mesons from the definition of the decay constant.

where the first (second) value corresponds to the lower (upper) end of the range for the Wilson coefficient C_2. In each case, parametric uncertainties from the K_1 decay constants (A4), $D_{(s)}$-decay constants from lattice-QCD $f_D = (212.15 \pm 1.45)$ MeV and $f_{D_s} = (248.83 \pm 1.27)$ MeV [13], masses, lifetimes [4] and Cabibbo-Kobayashi-Maskawa elements [14] are taken into account and added in quadrature. The parameter $\lambda_{D_{(s)}} \sim \Lambda_{\rm QCD}$ is poorly known and constitutes a major uncertainty in the SM predictions (10). Data on $D \to V\gamma$ branching ratios suggest a rather low value for λ_D [11]. We use 0.1 GeV as a benchmark value for both D and D_s mesons.

Despite its V-A structure in the SM, contributions to right-handed photons are expected, which we denote by $A_{R\,\rm SM}^{D_{(s)}}$. One possible mechanism responsible for $\lambda_\gamma^{D_{(s)}} \neq -1$ is a quark loop with an $\mathcal{O}_{1,2}$ insertion and the photon and a soft gluon attached [15], at least perturbatively also subject to GIM suppression [11]. Here, we do not need to attempt an estimate of such effects as we take the SM fraction of right- to left-handed photons from a measurement of $\mathcal{A}_{\rm UD}^{D^+}$ in $D^+ \to K_1^+\gamma$ decays, which has no FCNC contribution. (We neglect BSM effects in four-quark operators.)

U-spin breaking between D and D_s meson decays can split the photon polarizations in the SM. While obvious sources such as phase space and Cabibbo-Kobayashi-Maskawa factors can be taken into account in a straightforward manner, there are further effects induced by hadronic physics. Examples for parametric input are the decay constants and $\lambda_{D_{(s)}}$, as in (9). The former has known U-spin splitting of ~ 0.15 [13], and for the latter, as not much is known, we assume that the spectator quark flavor does not matter beyond that. A measurement of $D_s \to \rho^+\gamma$, which is a Cabibbo and color-allowed SM-like mode with branching ratios of order 10^{-3} [11] can put this to the test. Nominal U-spin breaking in charm decays is $\mathcal{O}(0.2$–$0.3)$, e.g., Refs. [16–18]; however, the situation for the photon polarization is favorable, as only the residual breaking on the ratio of the left-handed to right-handed amplitudes is relevant for the null test. In the BSM study, we work with U-spin breaking between r_{D+} and r_{Ds} within $\pm 20\%$.

C. BSM

Beyond the SM, the GIM suppression does not have to be at work in general, and the dipole coefficients can be significantly enhanced. Model-independently, the following constraints hold,

$$|C_7|, |C_7'| \lesssim 0.5, \tag{11}$$

obtained from $D \to \rho^0\gamma$ decays [11,19] and consistent with limits from $D \to \pi^+\mu\mu$ decays [12].

The corresponding NP contributions to $D_s \to K_1^+\gamma$ decays are given as

$$A_{L\,\rm NP}^{D_s} = m_c C_7 T^{K_1}, \qquad A_{R\,\rm NP}^{D_s} = m_c C_7' T^{K_1}, \tag{12}$$

where $T^{K_1} = T_1^{D_s \to K_1}(0)$ is the form factor for the $D_s \to K_1$ transition, defined in Appendix A.

From radiative B decay data [20]

$$\mathcal{B}(B \to K^{0*}(892)\gamma) = (41.7 \pm 1.2) \times 10^{-6}, \tag{13}$$

$$\mathcal{B}(B^+ \to K_1^+(1270)\gamma) = (43.8^{+7.1}_{-6.3}) \times 10^{-6}, \tag{14}$$

$$\mathcal{B}(B^+ \to K_1^+(1400)\gamma) = (9.7^{+5.4}_{-3.8}) \times 10^{-6}, \tag{15}$$

one infers that $T_1^{B\to K_1(1400)}/T_1^{B\to K_1(1270)} \simeq 0.5$ and $T_1^{B\to K_1(1270)}/T_1^{B\to K^*(892)} \simeq 1.1$. Using $T_1^{D_s\to K^*(892)} \simeq 0.7$ from a compilation in Ref. [11] points to $T^{K_1(1270)} \simeq 0.8$ and $T^{K_1(1400)} \simeq 0.4$. We use $T^{K_1(1270)} = 0.8$ and $m_c = 1.27$ GeV to estimate the BSM reach.

The SM plus NP decay amplitudes read

$$A_{L/R}^{D^+} = A_{L/R\,\rm SM}^{D^+}, \qquad A_{L/R}^{D_s} = A_{L/R\,\rm SM}^{D_s} + A_{L/R\,\rm NP}^{D_s}, \tag{16}$$

and

$$r_{D^+} = \left|\frac{A_{R\,\rm SM}^{D^+}}{A_{L\,\rm SM}^{D^+}}\right|, \qquad r_{D_s} = \left|\frac{m_c T^{K_1} C_7'^{\rm eff} + A_{R\,\rm SM}^{D_s}}{m_c T^{K_1} C_7^{\rm eff} + A_{L\,\rm SM}^{D_s}}\right|. \tag{17}$$

In Fig. 2, we illustrate BSM effects that show up in $\lambda_\gamma^{D_s}$ being different from $\lambda_\gamma^{D^+}$ for NP in C_7' with $C_7 = 0$ (green curves) and in C_7 with $C_7' = 0$ (red curves), within the constraints in (11) for the $K_1(1270)$, central values of input, and for $\lambda_{D_{(s)}} = 0.1$ GeV. We learn that NP in the left- or right-handed dipole operator can significantly change the polarization in D^+ decays from the one in D_s decays. Larger values of $\lambda_{D_{(s)}}$ and T^{K_1} and smaller values of f_{K_1} enhance the BSM effects.

III. $K_1 \to K\pi\pi$ DECAYS

Here, we provide input for the $K_1 \to K\pi\pi$ helicity amplitude $\mathcal{J}$, which drives the sensitivity to the photon polarization in the up-down asymmetry (5). After giving a general Lorentz decomposition, we resort to a phenomenological model for the form factors, which allows us to estimate $\mathcal{J}$ and sensitivities. This section is based on corresponding studies in B decays [2,21,22]. While it is relevant for the sensitivity, we recall that knowledge of $\mathcal{J}$ in charm decays is not needed as a theory input to perform the SM null test.

We consider two K_1 states, $K_1(1270)$ and $K_1(1400)$, with spin parity $J^{\mathcal{P}} = 1^+$. For the charged resonance K_1^+, two types of charge combinations exist for the final state, $K_1^+ \to K^0\pi^+\pi^0$ (channel I) and $K_1^+ \to K^+\pi^+\pi^-$ (channel II),

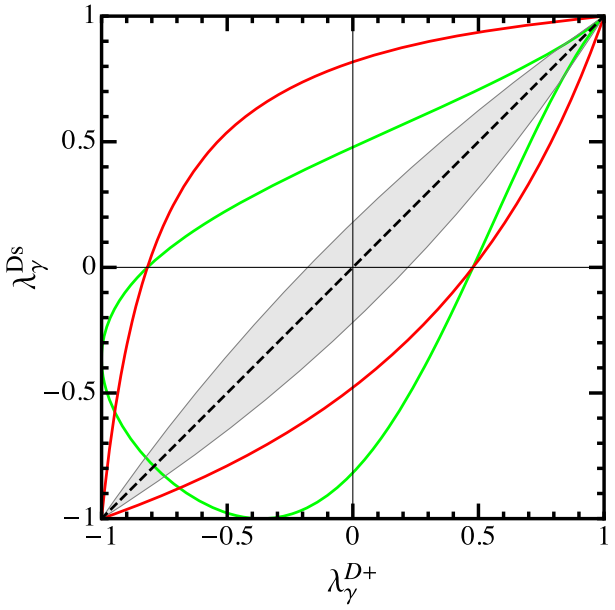

FIG. 2. BSM reach of $\lambda_\gamma^{D_s}$ for given $\lambda_\gamma^{D^+}$ for NP in C_7' (with $C_7 = 0$, green curves) and NP in C_7 (with $C_7' = 0$ red curves), within (11) for the $K_1(1270)$, central values of input, $f_{K_1} = 170$ MeV, $T^{K_1} = 0.8$, and for $\lambda_{D_{(s)}} = 0.1$ GeV. The black dashed line denotes the SM in the flavor limit, and the gray shaded area illustrates ±20% U-spin breaking between r_{D^+} and r_{D_s}.

$$\text{I: } K_1^+(1270/1400) \to \underbrace{\underbrace{\pi^0(p_1)\pi^+}_{\rho^+}(p_2)K^0}_{K^{*0}}{}^{K^{*+}}(p_3),$$
$$\text{II: } K_1^+(1270/1400) \to \underbrace{\underbrace{\pi^-(p_1)\pi^+}_{\rho^0}(p_2)K^+}_{K^{*0}}(p_3), \tag{18}$$

both of which we consider in the following.

The $K_1 \to K\pi\pi$ decay amplitude can be written in terms of the helicity amplitude $\mathcal{J}$ as

$$\mathcal{M}(K_{1L,R} \to K\pi\pi)^{I,II} = \varepsilon^\mu_{L,R}\mathcal{J}^{I,II}_\mu, \tag{19}$$

with the K_1 polarization vector $\varepsilon^\mu_{L,R} = (0, \pm 1, -i, 0)/\sqrt{2}$. For a 1^+ state, $\mathcal{J}^{I,II}_\mu$ can be parametrized by two functions, $\mathcal{C}_{1,2}$, as

$$\mathcal{J}^{I,II}_\mu = [\mathcal{C}_1^{I,II}(s, s_{13}, s_{23})p_{1\mu} - \mathcal{C}_2^{I,II}(s, s_{13}, s_{23})p_{2\mu}]BW_{K_1}(s). \tag{20}$$

From here on, assumptions are needed to make progress on the numerical predictions of the phenomenological profiles. First, the $\mathcal{C}_{1,2}$-functions are modeled by the quasi-two-body decays $K_1 \to K\rho(\to\pi\pi)$ and $K_1 \to K^*(\to K\pi)\pi$. Taking into account the isospin factors for each charge mode, $K_1^+ \to K^0\pi^+\pi^0$ and $K_1^+ \to K^+\pi^+\pi^-$, $\mathcal{C}^{I,II}_{1,2}$ can be rewritten in the following form [22],

$$\begin{aligned}
\mathcal{C}_1^I &= \frac{\sqrt{2}}{3}(a_{13}^{K^*} - b_{13}^{K^*}) + \frac{\sqrt{2}}{3}b_{23}^{K^*} + \frac{1}{\sqrt{3}}a_{12}^\rho,\\
\mathcal{C}_2^I &= \frac{\sqrt{2}}{3}b_{13}^{K^*} + \frac{\sqrt{2}}{3}(a_{23}^{K^*} - b_{23}^{K^*}) - \frac{1}{\sqrt{3}}b_{12}^\rho,\\
\mathcal{C}_1^{II} &= -\frac{2}{3}(a_{13}^{K^*} - b_{13}^{K^*}) - \frac{1}{\sqrt{6}}a_{12}^\rho,\\
\mathcal{C}_2^{II} &= -\frac{2}{3}b_{13}^{K^*} + \frac{1}{\sqrt{6}}b_{12}^\rho,
\end{aligned} \tag{21}$$

where

$$\begin{aligned}
a_{ij}^V &= g_{VP_iP_j}BW_V(s_{ij})[f^V + h^V\sqrt{s}(E_i - E_j) - \Delta_{ij}],\\
b_{ij}^V &= g_{VP_iP_j}BW_V(s_{ij})[-f^V + h^V\sqrt{s}(E_i - E_j) - \Delta_{ij}],
\end{aligned} \tag{22}$$

with $\Delta_{ij} = \frac{(m_i^2 - m_j^2)}{m_V^2}[f^V + h^V\sqrt{s}(E_i + E_j)]$, $E_i = \frac{(s - s_{i3} + m_i^2)}{2\sqrt{s}}$, and the Breit-Wigner shapes $BW_V(s_{ij}) = (s_{ij} - m_V^2 + im_V\Gamma_V)^{-1}$. The definitions of the form factors of the $K_1 \to VP$ ($V = K^*, \rho$ and $P = \pi$, K) decay, f^V, h^V, and decay constants of the $V \to P_iP_j$ decay, $g_{VP_iP_j}$ are given in Appendix B. The form factors are obtained in the Quark-Pair-Creation Model (QPCM) [23].

In the presence of two K_1 states, $K_1(1270)$ and $K_1(1400)$, this framework can be extended by adding the contributions weighted by the line shapes

$$\begin{aligned}
\mathcal{J}^{I,II}_\mu = \sum_{K_{\rm res}=K_1(1270,1400)} \xi_{K_{\rm res}}[&\mathcal{C}^{I,II}_{1K_{\rm res}}(s, s_{13}, s_{23})p_{1\mu}\\
&- \mathcal{C}^{I,II}_{2K_{\rm res}}(s, s_{13}, s_{23})p_{2\mu}]BW_{K_{\rm res}}(s),
\end{aligned} \tag{23}$$

and the parameter $\xi_{K_{\rm res}}$, which allows us to switch the states on and off individually. Importantly, in a generic situation with all K_1-resonances contributing, $\xi_{K_{\rm res}}$ takes into account the differences in their production in the weak decay. Such effects are induced by the K_1-dependence of hadronic matrix elements, such as $f_{K_1}m_{K_1}$ in (9) or T^{K_1} in (12). For $f_{K_1(1400)}m_{K_1(1400)}/(f_{K_1(1270)}m_{K_1(1270)}) \sim 1.1$ and $T^{K_1(1400)}/T^{K_1(1270)} \sim 0.5$, this effect is rather mild. The ansatz (23), which is an approximation of the general formula (C3), allows us to compute $\mathcal{A}_{\rm UD}/\lambda_\gamma$ as in (5) in Sec. IV independent of the weak decays. Equation (23) becomes exact, i.e., coincides with (C3) for universal $\xi_{K_{\rm res}}$.

Due to isospin, $\mathcal{I}m[\vec{n}\cdot(\vec{\mathcal{J}} \times \vec{\mathcal{J}}^*)]$ in the $K_1^+ \to K^0\pi^+\pi^0$ channel is antisymmetric in the (s_{13}, s_{23})-Dalitz plane. This can be seen explicitly by interchanging $s_{13} \leftrightarrow s_{23}$ in Eq. (21), which implies $\mathcal{C}_1 \leftrightarrow \mathcal{C}_2$, and therefore

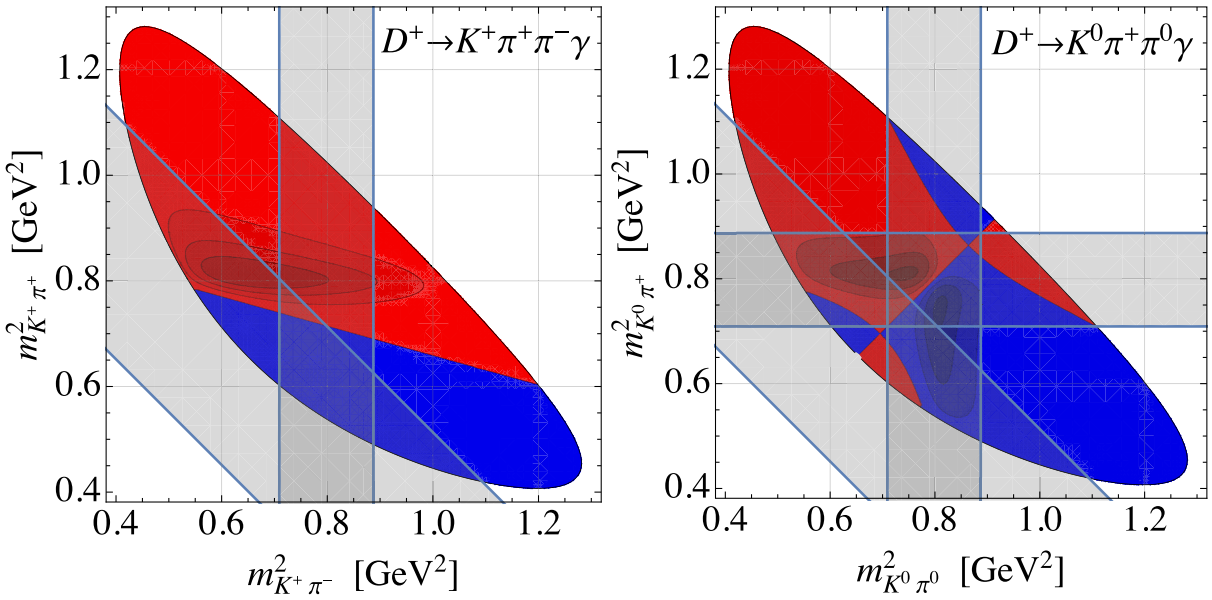

FIG. 3. Dalitz contour plots of $\mathcal{I}m[\vec{n}\cdot(\vec{\mathcal{J}}\times\vec{\mathcal{J}}^*)]$ for $K^+\pi^+\pi^-$ (plot to the left) and $K^0\pi^+\pi^0$ (plot to the right) at $m^2_{K\pi\pi} = m^2_{K_1(1270)}$. Red (blue) areas correspond to positive (negative) values of $\mathcal{I}m[\vec{n}\cdot(\vec{\mathcal{J}}\times\vec{\mathcal{J}}^*)]$. Grey bands represent the $K^*(\rho)$ resonance $[(m_{K^*(\rho)}-\Gamma_{K^*(\rho)})^2,(m_{K^*(\rho)}+\Gamma_{K^*(\rho)})^2]$ intervals.

$\mathcal{I}m[\vec{n}\cdot(\vec{\mathcal{J}}\times\vec{\mathcal{J}}^*)] \propto \mathcal{I}m[\mathcal{C}_1\mathcal{C}_2^*]$ changes sign when crossing the $s_{13}=s_{23}$ line; see the plot to the right in Fig. 3. Therefore, in order to have a nonzero up-down asymmetry after s_{13}, s_{23}-integration, one has to define the asymmetry with $\langle \mathrm{sgn}(s_{13}-s_{23})\mathcal{I}m[\vec{n}\cdot(\vec{\mathcal{J}}\times\vec{\mathcal{J}}^*)]\rangle$ in Eq. (5). In the $K_1^+\to K^+\pi^-\pi^+$ channel and with only one K_1, the border, at which $\mathcal{A}_{\mathrm{UD}}$ changes sign, is a straight line in the (s_{13},s_{23})-plane, see the plot to the left in Fig. 3, which is described by $\mathcal{I}m[BW_{K^*}(s_{13})BW^*_\rho(s_{12})]=0$. The location of this line in the Dalitz plane depends on s via $s=s_{12}+s_{23}+s_{13}+2m_\pi^2+m_K^2$.

IV. UP-DOWN ASYMMETRY PROFILES

In the following, we work out estimates for the up-down asymmetry in units of the photon polarization parameter $\mathcal{A}_{\mathrm{UD}}/\lambda_\gamma$, as in (5). The crucial ingredient for probing the photon polarization is the hadronic factor $\mathcal{I}m[\vec{n}\cdot(\vec{\mathcal{J}}\times\vec{\mathcal{J}}^*)]$. Using (23), and for two interfering resonances a, b, e.g., $a=K_1(1270)$ and $b=K_1(1400)$, dropping channel I,II superscripts and kinematic variables to ease notation, it reads

$$\begin{aligned}&\mathcal{I}m[\vec{n}\cdot(\vec{\mathcal{J}}\times\vec{\mathcal{J}}^*)]\\&\quad=-2\mathcal{I}m[\xi_a^2\mathcal{C}_{1a}\mathcal{C}_{2a}^*|BW_a|^2+\xi_b^2\mathcal{C}_{1b}\mathcal{C}_{2b}^*|BW_b|^2\\&\qquad+\xi_a\xi_b(\mathcal{C}_{1a}\mathcal{C}_{2b}^*-\mathcal{C}_{1b}\mathcal{C}_{2a}^*)BW_aBW_b^*]|\vec{p}_1\times\vec{p}_2|,\end{aligned}\tag{24}$$

which shows the necessity of having relative strong phases for a nonzero up-down asymmetry. Such phases can come from the interference between $K^*\pi$ and $K\rho$ channels inside of $\mathcal{C}_{1,2}$, as well as from the interference between the K_1 resonances. Due to the larger number of interfering amplitudes (18), we quite generally expect larger phases in the $K_1^+\to K^0\pi^+\pi^0$ channel. While the $K_1(1270)$ decays to both $K\rho$ and $K^*\pi$, the $K_1(1400)$ decays predominantly to $K^*\pi$. We therefore expect the pure $K_1(1400)$ contribution to $\mathcal{A}_{\mathrm{UD}}/\lambda_\gamma$ in the $K^+\pi^+\pi^-$ channel to be very small.

In Fig. 4, we show the $m_{K\pi\pi}$-dependence of $|\vec{\mathcal{J}}|^2$ (plots to the left) and $\mathcal{A}_{\mathrm{UD}}/\lambda_\gamma$ (plots to the right). The different colors refer to different ratios of the $K_1(1270)$ and $K_1(1400)$ contributions. Specifically, black, red, green, and magenta lines correspond to $\xi_{K_1(1400)}=0,+0.5,+1$, and -1, respectively, for fixed $\xi_{K_1(1270)}=1$. The blue curve refers to only the $K_1(1400)$ being present, with $\xi_{K_1(1270)}=0$. Upper (lower) plots are for channel II (channel I).

The measured invariant mass $m_{K\pi\pi}$ spectrum in $B^+\to K^+\pi^+\pi^-\gamma$ decays [24–26] exhibits the dominant $K_1(1270)$ peak along with a $K_1(1400)$ shoulder, plus higher resonances. For our model, these measurements suggest a value of $\xi_{K_1(1400)}/\xi_{K_1(1270)}$ around $+1$, see Fig. 4, consistent with expectations based on small K_1-dependence; see Sec. III. We also note that resonances higher than the $K_1(1270)$ and the $K_1(1400)$, such as the $K_2^\star(1430)(2^+)$ and the $K^*(1410)(1^-)$, which are not taken into account in our analysis, contribute. Our predictions therefore oversimplify the situation for $m_{K\pi\pi}\gtrsim 1400$ MeV.

Since the up-down asymmetry is sensitive to complex phases in the K_1 decay amplitudes, we test several possible sources apart from the ones coming from the Breit-Wigner functions of the K_1, K^* and the ρ. As expected, it turns out

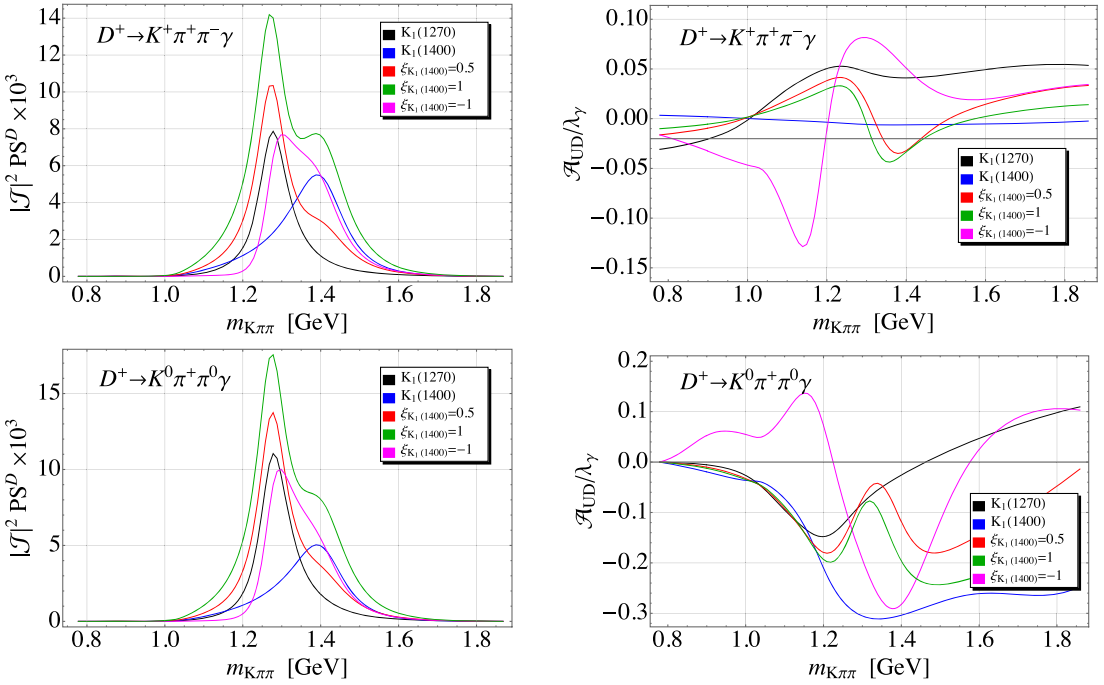

FIG. 4. Invariant $K^+\pi^+\pi^-$ (upper plots) and $K^0\pi^+\pi^0$ (lower plots) mass dependence of $|\vec{\mathcal{J}}|^2$ (plots to the left), multiplied by the four-body phase space factor (4), and $\mathcal{A}_{\mathrm{UD}}/\lambda_\gamma$ (plots to the right) for $K_1(1270, 1400)$ resonances separately and with relative fraction of the $K_1(1400)$ contribution, $\xi_{K_1(1400)}$; see the text for details.

that such phases have only a negligible effect on the $|\vec{\mathcal{J}}|^2$ distributions, and we do not show corresponding plots. The Belle Collaboration in the analysis of $B^+ \to J/\psi K^+\pi^+\pi^-$ and $B^+ \to \psi' K^+\pi^+\pi^-$ decays signals a nonzero phase,

$$\delta_\rho = \arg\left[\frac{\mathcal{M}(K_1(1270)\to(K\rho)_S)\times\mathcal{M}(\rho\to\pi\pi)}{\mathcal{M}(K_1(1270)\to(K^*\pi)_S)\times\mathcal{M}(K^*\to K\pi)}\right], \quad (25)$$

as $\delta_\rho = -(43.8 \pm 4.0 \pm 7.3)^\circ$ [24]. A similar value was found in the reanalysis of the ACCMOR data [27] by the *BABAR* Collaboration, as $\delta_\rho = (-31 \pm 1)^\circ$ [28]. Therefore, we add an additional phase $\delta_\rho = -40^\circ$ to the $K\rho$ S-wave[2] amplitude and consider it theoretical uncertainty. The effect of this additional phase in $\mathcal{A}_{\mathrm{UD}}$ (dashed curves) in comparison with the QPCM predictions (solid curves) is presented in Fig. 5. We also investigate the impact of the additional phase $\delta_D = \arg[\mathcal{M}(K_1(1270)\to(K^*\pi)_D)/\mathcal{M}(K_1(1270)\to(K^*\pi)_S)] = 90^\circ$. The result can be seen in Fig. 6. Note that δ_ρ and δ_D vanish in the QPCM and are therefore termed offset phases.

We learn from Figs. 4–6 that $\mathcal{A}_{\mathrm{UD}}/\lambda_\gamma$ profiles with $\xi_{K_1(1400)} = 0.5$, 1 (red and green curves, respectively) can be of the orders of ~ 0.05–0.1 (channel II) and ~ 0.2–0.3 (channel I), which are, as expected, larger for $K^0\pi^+\pi^0$ than for $K^+\pi^+\pi^-$ final states. Adding phenomenological strong phases such as δ_ρ and δ_D has a significant effect for channel II. As zero-crossings can occur it may be disadvantageous to not use $m_{K\pi\pi}$ bins, in particular, for channel II. The position of the zeros, however, cannot be firmly predicted, although the one at $m_{K^+\pi^+\pi^-} \simeq 1$ GeV, whose origin is discussed at the end of Sec. III, is quite stable, as well as the one at $m_{K^+\pi^+\pi^-} \simeq 1.3$ GeV. The latter stems from $K_1(1270)$ and $K_1(1400)$ interference.

Strong phases and, related to this, K_1-mixing constitute the main sources of uncertainty. Figures 4–6 are obtained for fixed mixing angle $\theta_{K_1} = 59^\circ$; see Appendix B. Varying θ_{K_1} within its 1σ range, $\pm 10^\circ$, determined within the QPCM, as well as $\delta_D \in [0, 2\pi]$ for $\delta_\rho = 0, -40^\circ$, we find for the $m_{K\pi\pi}$-integrated up-down asymmetry assuming $K_1(1270)$ dominance the ranges $[-30, +2]\%$ (channel I) and $[+2, +13]\%$ (channel II). Recall that the latter exhibits cancellations so that locally the asymmetry can be larger. Our results are compatible with the findings $[-10, -7]\%$ (channel I) and $[-13, +24]\%$ (channel II) of Ref. [29], which are based on $K_1(1270)$ dominance. Note that Ref. [29] uses $\kappa = \mathrm{sgn}(s_{13} - s_{23})$ for both channels. Our prediction for channel II in this convention reads $[-18, +8]\%$.

We stress that the estimates are subject to sizable uncertainties and serve as a zeroth order study to explore the BSM potential in $D_s \to K_1\gamma$ decays. $K\pi\pi$ profiles from the B-sector can be linked to charm physics, and vice versa.

[2]Due to the smallness of the $K\rho$ D-wave amplitude, we neglect its contribution in our study.

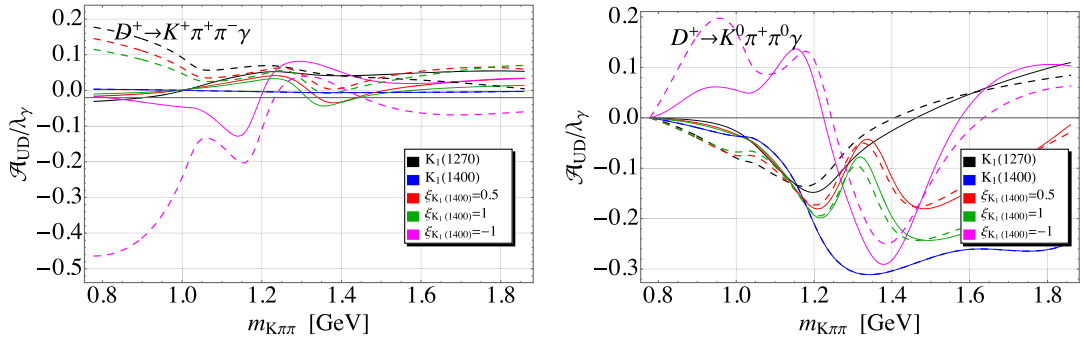

FIG. 5. Invariant $K^+\pi^+\pi^-$ (plot to the left) and $K^0\pi^+\pi^0$ (plot to the right) mass dependence of $\mathcal{A}_{\rm UD}/\lambda_\gamma$ for $K_1(1270, 1400)$ resonances separately and with the relative fraction of the $K_1(1400)$ contribution, $\xi_{K_1(1400)}$. Solid lines correspond to all "offset" phases equal to zero, i.e., the pure quark model prediction. Dashed lines represent the offset phase $\delta_\rho = \arg[\mathcal{M}(K_1(1270) \to K\rho)_S/\mathcal{M}(K_1(1270) \to (K^*\pi)_S)] = -40°$.

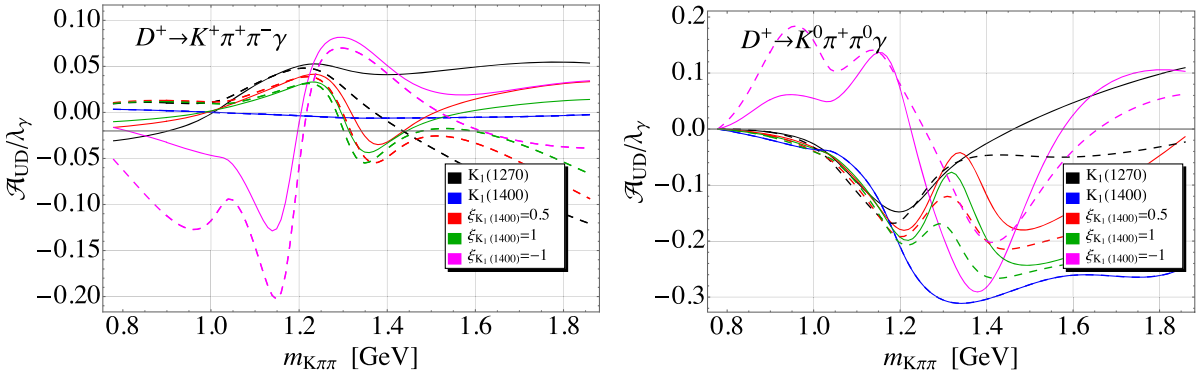

FIG. 6. The same as Fig. 5 for $\delta_\rho = 0$ and with dotted lines representing the offset phase $\delta_D = \arg[\mathcal{M}(K_1(1270) \to (K^*\pi)_D)/\mathcal{M}(K_1(1270) \to (K^*\pi)_S)] = 90°$.

V. CONCLUSIONS

New physics may be linked to flavor, and K, D, and B systems together are required to decipher its family structure. Irrespective of this global picture, SM tests in semileptonic and radiative $c \to u$ transitions are interesting *per se* and quite unexplored territory today; present bounds on short-distance couplings are about 2 orders of magnitude away from the SM [11,12].

We study a null test of the SM in radiative rare charm decays based on the comparison of the up-down asymmetry in $D^+ \to K_1^+(\to K\pi\pi)\gamma$, which is SM-like, to the one in $D_s \to K_1^+(\to K\pi\pi)\gamma$, which is a FCNC. The up-down asymmetry depends on the photon polarization, subject to BSM effects in the $|\Delta c| = |\Delta u| = 1$ transition.

We find that, model-independently, NP in photonic dipole operators can alter the polarization of $D_s \to K_1^+(\to K\pi\pi)\gamma$ from the SM value at order one level; see Fig. 2. We estimate the proportionality factor between the integrated up-down asymmetry (5) and the polarization parameter to be up to $\mathcal{O}$(5–10)%, and 40% in extreme cases, for $K_1^+ \to K^+\pi^+\pi^-$ and $\mathcal{O}$(20–30)% for $K_1^+ \to K^0\pi^+\pi^0$, respectively; see Figs. 4–6. As in previous studies carried out for $B \to K_1^+(\to K\pi\pi)\gamma$ decays, there are sizable uncertainties associated with these estimates. Unlike in B-physics, these do not affect the SM null test. With branching ratios (10) of $\mathcal{B}(D^+ \to K_1^+\gamma)$ of $\mathcal{O}(10^{-5})$ and $\mathcal{B}(D_s \to K_1^+\gamma)$ of $\mathcal{O}(10^{-4})$, analyses of up-down asymmetries in the charm sector constitute an interesting NP search for current and future flavor facilities.

ACKNOWLEDGMENTS

We are grateful to Stefan de Boer and Emi Kou for useful discussions and comments on the manuscript. This work has been supported by the DFG Research Unit FOR 1873 "Quark Flavour Physics and Effective Field Theories."

APPENDIX A: MATRIX ELEMENTS

The matrix element of the electromagnetic dipole operator can be parametrized as

$$\begin{aligned}\langle K_1(\varepsilon,k)|\bar{u}\sigma_{\mu\nu}(1\pm\gamma_5)q^\nu c|D_s(p)\rangle &= T_2^{K_1}(q^2)[\varepsilon_\mu^*(m_{D_s}^2-m_{K_1}^2)-(\varepsilon^* p)(p+k)_\mu] \\ &+ T_3^{K_1}(q^2)(\varepsilon^* p)\left[q_\mu-\frac{q^2}{m_{D_s}^2-m_{K_1}^2}(p+k)_\mu\right] \\ &\pm 2T_1^{K_1}(q^2)i\epsilon_{\mu\nu\rho\sigma}\varepsilon^{\nu *}p^\rho k^\sigma, \end{aligned} \tag{A1}$$

with $T_1^{K_1}(0)=T_2^{K_1}(0)$.

The K_1 and $D_{(s)}$ decay constants are defined as

$$\langle K_1(\varepsilon,k)|\bar{u}\gamma_\mu\gamma_5 s|0\rangle = f_{K_1} m_{K_1}\varepsilon_\mu^*, \tag{A2}$$

$$\langle 0|\bar{d}(\bar{s})\gamma_\mu\gamma_5 c|D_{(s)}(p)\rangle = i f_{D_{(s)}} p_\mu. \tag{A3}$$

We employ the following values for the K_1 decay constants:

$$\begin{aligned} f_{K_1(1270)} &= (170\pm 20)\ \text{MeV}, \\ f_{K_1(1400)} &= (175\pm 37)\ \text{MeV}. \end{aligned} \tag{A4}$$

Here, $f_{K_1(1270)}$ is extracted from $\mathcal{B}(\tau^-\to K_1(1270)^-\nu_\tau)^{\text{exp}} = (4.7\pm 1.1)\times 10^{-3}$ [4], as

$$\mathcal{B}(\tau\to K_1\nu_\tau)=\tau_\tau\frac{G_F^2}{16\pi}|V_{us}|^2 f_{K_1}^2 m_\tau^3\left(1+\frac{2m_{K_1}^2}{m_\tau^2}\right)\left(1-\frac{m_{K_1}^2}{m_\tau^2}\right)^2. \tag{A5}$$

The value of $f_{K_1(1270)}$ from a light cone sum rule calculation [30] is consistent with the data-based value (A4) assuming the SM. The value of $f_{K_1(1400)}$ is taken from Ref. [30]; we added statistical and systematic uncertainties in quadrature and symmetrized the uncertainties. $\mathcal{B}(\tau^-\to K_1(1400)^-\nu_\tau)^{\text{exp}} = (1.7\pm 2.6)\times 10^{-3}$ [4] has too large an uncertainty to allow for an extraction of $f_{K_1(1400)}$ but yields a 90% C.L. upper limit as $|f_{K_1(1400)}| < 235$ MeV, consistent with (A4).

APPENDIX B: $K_1 \to VP$ FORM FACTORS

The hadronic form factors, f_V and h_V, defined as

$$\mathcal{M}(K_1\to VP) = \varepsilon_{K_1}^\mu(f^V g_{\mu\nu}+h^V p_{V\mu}p_{K_1\nu})\varepsilon_V^{\nu *}, \tag{B1}$$

are related to the partial S, D wave amplitudes,

$$\begin{aligned} f^V &= -A_S^V-\frac{1}{\sqrt{2}}A_D^V, \\ h^V &= \frac{E_V}{\sqrt{s}|\vec{p}_V|^2}\left[\left(1-\frac{\sqrt{s_V}}{E_V}\right)A_S^V+\left(1+2\frac{\sqrt{s_V}}{E_V}\right)\frac{1}{\sqrt{2}}A_D^V\right]. \end{aligned} \tag{B2}$$

These partial wave amplitudes are computed in the framework of the $^3P_0$ QPCM [23]. The details of the computation and expressions for $A_{S,D}^{K^*/\rho}$ can be found in Ref. [22].

The $g_{VP_iP_j}$ couplings can be extracted from the partial decay width of the vector mesons,

$$\Gamma(V\to P_iP_j)=\frac{g_{VP_iP_j}^2}{2\pi M_V^2}|\vec{p}|^3\frac{1}{3}, \tag{B3}$$

where $|\vec{p}|=\sqrt{(m_V^2-(m_i+m_j)^2)(m_V^2-(m_i-m_j)^2)}/2m_V$. Using the experimental values of the ρ and K^* widths, we find $g_{\rho\pi\pi}=-(5.98\pm 0.02)$, $g_{K^*K\pi}=5.68\pm 0.05$ with the relative sign fixed by QPCM; see Ref. [22] for details.

Due to $SU(3)$ breaking, the $K_1(1270)$ and $K_1(1400)$ mesons are an admixture of the spin singlet and triplet P-wave states $K_{1B}(1^1P_1)$ and $K_{1A}(1^3P_1)$, respectively,

$$|K_1(1270)\rangle = |K_{1A}\rangle\sin\theta_{K_1}+|K_{1B}\rangle\cos\theta_{K_1}, \tag{B4}$$

$$|K_1(1400)\rangle = |K_{1A}\rangle\cos\theta_{K_1}-|K_{1B}\rangle\sin\theta_{K_1}, \tag{B5}$$

with mixing angle $\theta_{K_1}=(59\pm 10)^\circ$ [22], which has been obtained from $K_1\to VP$ decay data.

APPENDIX C: GENERAL FORMULA FOR THE UP-DOWN ASYMMETRY

The reduced amplitude of $D_{(s)}\to K_{\text{res}}\gamma\to K\pi\pi\gamma$ decays can be written as the product of the weak decay amplitude $\mathcal{M}_{L/R}^{D_{(s)},K_{\text{res}}}$ and strong decay amplitude $\mathcal{J}_\mu^{K_{\text{res}}}$ as

$$\mathcal{G}_{\mu,L/R}^{D_{(s)}}=\sum_{K_{\text{res}}}\mathcal{M}_{L/R}^{D_{(s)},K_{\text{res}}}\mathcal{J}_\mu^{K_{\text{res}}}. \tag{C1}$$

Multiplying $\mathcal{G}_{\mu,L/R}^{D_{(s)}}$ by the photon polarization vector and integrating over azimuthal angles, we obtain the general formula for modulus squared of the matrix element,

$$\begin{aligned}\overline{|\mathcal{M}^{D_{(s)}}|^2} \propto{}& (|\vec{\mathcal{G}}_L^{D_{(s)}}|^2+|\vec{\mathcal{G}}_R^{D_{(s)}}|^2)(1+\cos^2\theta) \\ &-2\mathcal{I}m[\vec{n}\cdot(\vec{\mathcal{G}}_L^{D_{(s)}}\times\vec{\mathcal{G}}_L^{D_{(s)}*}-\vec{\mathcal{G}}_R^{D_{(s)}}\times\vec{\mathcal{G}}_R^{D_{(s)}*})]\cos\theta. \end{aligned} \tag{C2}$$

This expression holds even beyond (C1), such as for nonresonant contributions, as long as the $K\pi\pi$ system is in the same spin, parity state as K_{res}, 1^+. The up-down asymmetry then reads

$$\begin{aligned}\mathcal{A}_{\text{UD}}^{D_{(s)}} &= \frac{[\int_0^1-\int_{-1}^0]\frac{d^2\Gamma^{D_{(s)}}}{ds\,d\cos\theta}d\cos\theta}{\int_{-1}^1\frac{d^2\Gamma^{D_{(s)}}}{ds\,d\cos\theta}d\cos\theta} \\ &= -\frac{3}{4}\frac{\langle\mathcal{I}m[\vec{n}\cdot(\vec{\mathcal{G}}_L^{D_{(s)}}\times\vec{\mathcal{G}}_L^{D_{(s)}*}-\vec{\mathcal{G}}_R^{D_{(s)}}\times\vec{\mathcal{G}}_R^{D_{(s)}*})]\rangle}{\langle|\vec{\mathcal{G}}_L^{D_{(s)}}|^2+|\vec{\mathcal{G}}_R^{D_{(s)}}|^2\rangle}. \end{aligned} \tag{C3}$$

[1] M. Gronau, Y. Grossman, D. Pirjol, and A. Ryd, Phys. Rev. Lett. **88**, 051802 (2002).
[2] M. Gronau and D. Pirjol, Phys. Rev. D **66**, 054008 (2002).
[3] S. de Boer and G. Hiller, Eur. Phys. J. C **78**, 188 (2018).
[4] M. Tanabashi *et al.* (Particle Data Group), Phys. Rev. D **98**, 030001 (2018).
[5] A. Khodjamirian, G. Stoll, and D. Wyler, Phys. Lett. B **358**, 129 (1995).
[6] S. Fajfer, S. Prelovsek, and P. Singer, Eur. Phys. J. C **6**, 471 (1999).
[7] J. Lyon and R. Zwicky, arXiv:1210.6546.
[8] J. Gratrex and R. Zwicky, J. High Energy Phys. 08 (2018) 178.
[9] M. Beneke, G. Buchalla, M. Neubert, and C. T. Sachrajda, Nucl. Phys. **B591**, 313 (2000).
[10] S. W. Bosch and G. Buchalla, Nucl. Phys. **B621**, 459 (2002).
[11] S. de Boer and G. Hiller, J. High Energy Phys. 08 (2017) 091.
[12] S. de Boer and G. Hiller, Phys. Rev. D **93**, 074001 (2016).
[13] S. Aoki *et al.*, Eur. Phys. J. C **77**, 112 (2017).
[14] M. Bona *et al.* (UTfit Collaboration), J. High Energy Phys. 10 (2006) 081.
[15] B. Grinstein, Y. Grossman, Z. Ligeti, and D. Pirjol, Phys. Rev. D **71**, 011504 (2005).
[16] J. Brod, Y. Grossman, A. L. Kagan, and J. Zupan, J. High Energy Phys. 10 (2012) 161.
[17] G. Hiller, M. Jung, and S. Schacht, Phys. Rev. D **87**, 014024 (2013).
[18] S. Müller, U. Nierste, and S. Schacht, Phys. Rev. D **92**, 014004 (2015).
[19] A. Abdesselam *et al.* (Belle Collaboration), Phys. Rev. Lett. **118**, 051801 (2017).
[20] Y. Amhis *et al.* (HFLAV Collaboration), Eur. Phys. J. C **77**, 895 (2017).
[21] E. Kou, A. Le Yaouanc, and A. Tayduganov, Phys. Rev. D **83**, 094007 (2011).
[22] A. Tayduganov, E. Kou, and A. Le Yaouanc, Phys. Rev. D **85**, 074011 (2012).
[23] A. Le Yaouanc, L. Oliver, O. Pene, and J. C. Raynal, Phys. Rev. D **8**, 2223 (1973).
[24] H. Guler *et al.* (Belle Collaboration), Phys. Rev. D **83**, 032005 (2011).
[25] R. Aaij *et al.* (LHCb Collaboration), Phys. Rev. Lett. **112**, 161801 (2014).
[26] P. del Amo Sanchez *et al.* (*BABAR* Collaboration), Phys. Rev. D **93**, 052013 (2016).
[27] C. Daum *et al.* (ACCMOR Collaboration), Nucl. Phys. **B187**, 1 (1981).
[28] B. Aubert *et al.* (*BABAR* Collaboration), Phys. Rev. D **81**, 052009 (2010).
[29] M. Gronau and D. Pirjol, Phys. Rev. D **96**, 013002 (2017).
[30] H. Hatanaka and K. C. Yang, Phys. Rev. D **77**, 094023 (2008); **78**, 059902(E) (2008).